

# Generating coupled cluster code for modern distributed memory tensor software

Jan Brandejs <sup>a)</sup>, Johann Pototschnig , and Trond Saue 

Laboratoire de Chimie et Physique Quantique, UMR 5626 CNRS — Université Toulouse III-Paul Sabatier, 118 route de Narbonne, F-31062 Toulouse, France

(Dated: 12 September 2024)

Scientific groups are struggling to adapt their codes to quickly-developing GPU-based HPC platforms. The domain of distributed coupled cluster (CC) calculations is not an exception. Moreover, our applications to tiny QED effects require higher-order CC which include thousands of tensor contractions, which makes automatic treatment imperative. The challenge is to allow efficient implementation by capturing key symmetries of the problem, while retaining the abstraction from the hardware. We present the tensor programming framework tenpi, which seeks to find this balance. It features a python library user interface, global optimization of intermediates, a visualization module and Fortran code generator that bridges the DIRAC package for relativistic molecular calculations to tensor contraction libraries. tenpi brings higher-order CC functionality to the massively parallel module of DIRAC. The architecture and design decision schemes are accompanied by benchmarks and by first production calculations on Summit, Frontier and LUMI along with state-of-the-art of tensor contraction software.

## I. INTRODUCTION

According to Jack Dongarra, the cofounder of the TOP500 list, 99% of the FLOP performance of modern supercomputers lies in GPU accelerators.<sup>1,2</sup> However, in the domain of distributed coupled cluster calculations, which is the focus of the present work, most implementations are able to use only about 10% of the theoretical maximum FLOP rate.<sup>3</sup>

This exposes the difficult situation in which scientists find themselves.<sup>4,5</sup> Writing down fixed BLAS and MPI statements is no longer sufficient as modern machines have heterogeneous structures.<sup>6</sup> Figure 1 contains a schematic representation of a node of the Summit supercomputer. Communication throughputs and memory sizes differ substantially within and among the machines. Restructuring data movement across multiple levels of hierarchy to reduce the cost is a challenging problem,<sup>4</sup> where the developer basically faces a graph theoretical task.<sup>7</sup> The traditional 5-year lifespan of supercomputers<sup>8</sup> has accelerated to about 3 years due to AI-driven breakthroughs in energy efficiency<sup>9</sup> and keeping up with the changes requires expert manpower for which academia competes with industry.<sup>5,10</sup>

This develops a pressure on systematic treatment of the development.<sup>4,12–14</sup> One way is to build the code such that it can be quickly adapted to underlying numerical software changes using a code generator.<sup>12–14</sup> Another way is to rely on tools which allow a high level of abstraction, like MATLAB,<sup>15</sup> Maple<sup>16</sup> or Mathematica,<sup>17</sup> to write in parallel frameworks like SYCL<sup>18</sup> and OpenACC,<sup>19</sup> to use runtime environments like StarPU,<sup>20</sup> MADNESS<sup>21</sup> and LEGION,<sup>22</sup> or tensor compilers like DISTAL.<sup>23</sup>

In any case, one tries to i) abstract from hardware-specific code by using a high-level representation of the problem: creation/annihilation operator strings,<sup>12</sup> their expansion using Wick's theorem,<sup>24</sup> diagrams,<sup>25</sup> tensor operations,<sup>26</sup> portable

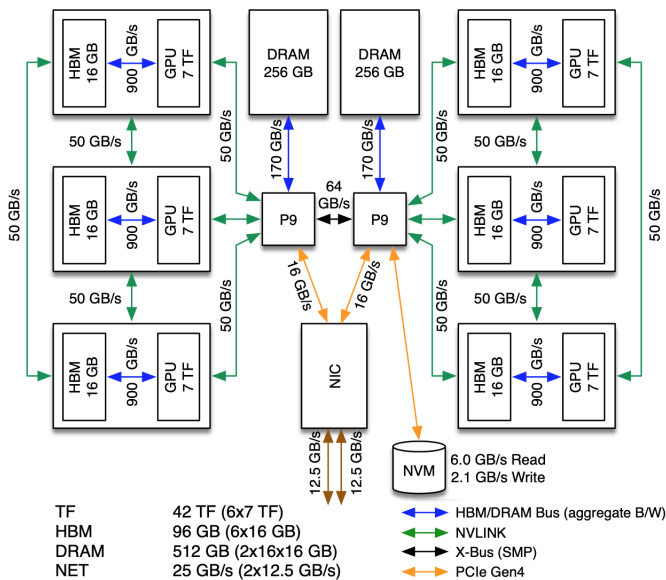


FIG. 1. Summit node structure. This figure is without copyright and is used after explicit consent by OLCF.<sup>11</sup>

tasks<sup>20</sup> and data distribution schemes.<sup>23</sup> ii) The software then translates this to instructions for hardware.

The challenge is to allow efficient implementation by capturing key mathematical symmetries of the problem, while retaining the abstraction from the hardware.<sup>27</sup> Strong candidates for finding this balance are tensor compilers<sup>23</sup> which have seen an explosion of interest<sup>28</sup> in the computer science (CS) community. However, to enable production use by chemists, performance-critical features like index permutation symmetry or block sparsity would need to be implemented.<sup>25,29</sup> The same holds for major machine learning libraries. Unlike in the case of AI, where big tech companies drive the development, in coupled cluster and tensor networks, scientists are left to rely on themselves. This was concluded by the representatives of big technology companies at the CECAM workshop<sup>30</sup>

<sup>a)</sup>Electronic mail: [jbrandejs@irsamc.ups-tlse.fr](mailto:jbrandejs@irsamc.ups-tlse.fr)

which we organized on the topic.

The purpose of this paper is to explore the path from the high-level representation of CC methods to an efficient code on modern machines and to provide the reader with a state-of-the-art on the necessary tensor software.

### A. Elegant development of CC methods, systematic approach

Equations in coupled cluster theory can reach a degree of complexity where manual manipulation is no longer practical. Higher orders of the method with quadruple excitations and above required for accurate applications include hundreds of terms with many indices. Even though derivation by hand can be simplified by using diagrams which help detect equivalent terms, further manipulations like the design of intermediates with respect to a given cost-function<sup>31</sup>, implementing other flavors of the method or verifying the correctness of the derivation steps are very error-prone when done by hand and hence are clear candidates for automatic symbolic treatment, which can speed up the implementation significantly.

There have been numerous efforts in this direction with differing degrees of success. Here we focus on complete toolchains which include both equation and code generation - these are often linked to an existing quantum chemistry package. A prominent example and one of the pioneering systematization efforts is the Tensor Contraction Engine (TCE)<sup>32</sup> initially developed by Hirata,<sup>14</sup> a part of NWChem software.<sup>33</sup> Even though TCE was not the such code generator,<sup>34-37</sup> to the best of our knowledge, it has the most complete description in literature.<sup>12</sup> Numerous works follow its scheme:<sup>25</sup>

1. Derivation (Derive the formulas of the method.)
2. Optimization (Optimize the expressions to reduce computational complexity.)
3. Transformation (Map to binary tensor contractions of a math library.)

Another noteworthy abstraction effort is the domain specific language (DSL) for tensor operations SIAL (superinstruction assembly language) in the ACES III package.<sup>26,38</sup> Even though initially successful, its limitation was the same as that of TCE: customizability. Not all CC methods can be expressed in the form of tensor contraction expressions and without C++ or Fortran frontend support, one could not easily include custom code and optimizations.<sup>29</sup> Further packages using their own tensor DSL include QChem<sup>39</sup> based on the libtensor<sup>40</sup> library, and Cyclops CTF<sup>41</sup> whose performance for distributed CPU contractions gained fame in the computer science community, where it is used as a reference.<sup>23,42,43</sup>

Formula generators themselves divide in three main groups based on their approach to the derivation: by applying the algebra of creation and annihilation operators, by Wick's theorem or diagrams.

Unlike TCE, which was based on Wick's theorem, the derivation inside the MRCC package of Kállay and Surján<sup>36</sup> uses a representation of Kucharski-Bartlett diagrams<sup>44,45</sup>

based on strings of integers. In terms of derivation, the present paper builds on their approach.

The SMITH generator of Shiozaki<sup>25,46</sup> is based on anti-symmetrized Goldstone diagrams.<sup>45,47</sup> SMITH comes with an elegant input format in terms of second-quantized operators sandwiched between Slater determinants. Compared to its predecessors, SMITH is able to produce intermediates with index permutation symmetry for a broader class of methods.<sup>25</sup> The latest version 3 has transitioned from Wick's theorem to second-quantized operators and was used to generate parts of the BAGEL package.<sup>48</sup>

Recent ORCA<sup>49</sup> is good example of a large-scale systematization effort where a substantial part of the package is generated using the ORCA-AGE generator<sup>12</sup> based directly on application of the algebra of creation and annihilation operators. Even though this approach is very general, it took up to 7 years to resolve performance issues with the generation.<sup>12,50</sup>

New efforts have emerged in past years, as groups behind quantum chemical packages consider having their own toolchain. Most of them use Wick's theorem: SeQuant of the Valeev group<sup>24</sup> which is a C++ rewrite of their Mathematica code, Drudge/Gristmill of the Scuseria group<sup>51</sup> which can switch between different abstract algebras and where the use of Wick's theorem is optional, FEMTO of Saitow<sup>52</sup> used for DMRG-MRCI and pair-natural orbitals, SQA<sup>53</sup> and GeCCo.<sup>54</sup> These efforts can be further classified by supported methods and features, see more detailed reviews.<sup>12,55</sup> Many other efforts exist which focus on only one of the three steps of the process.<sup>35,56-58</sup>

### B. Optimization step

The most difficult part of the entire process is the design of intermediates. This problem has not only proven to be NP-hard,<sup>12,59</sup> but in practice the actual cost-function depends on the model system, the hardware and the underlying math library. Instead, most optimizers rely on a naive FLOP count cost model, despite the fact that in the communication-heavy distributed CC calculations, this is not even the leading term. Most chemistry packages use just basic heuristics of single-term contraction path optimization and do not implement multi-term optimization for which they rely on hand-tuning.

The TCE also relies on performance model-driven search-based approach to program transformation, using a global optimizer OpMin written by Sadayappan.<sup>31</sup> The optimization consists of:

1. Single term optimization (contraction path within a term)
2. Factorization (distributive law)
3. Common subexpression elimination (reuse equivalent terms)

which later became a typical structure. OpMin performs well compared with hand-tuned code of NWChem for higher-order CC also thanks to its index-permutation-symmetry-awareness. But it does not support perturbative approaches with energy denominators.

Other efforts include a distributed GPU-contraction optimizer<sup>4</sup> benchmarked for CCSD(T), followed by the AutoHOOT optimizer<sup>60</sup> (not CC), and an optimizer with a GPU-aware cost model.<sup>61</sup> The aforementioned complete toolchains also include own optimizers of varying levels of sophistication. For more information, see the literature overview in the thesis of Panyala<sup>29</sup> on loop-level optimization.<sup>62,63</sup> Note that there is no clear boundary on how low-level an optimizer should be. If it reaches too low-level, it becomes a compiler, which is in fact a trend in state-of-the-art works.<sup>23,64</sup> Despite a strong connection to compiler optimizations for different applications,<sup>65–67</sup> these cannot be directly applied to tensor contractions in CC due to their distinctive features<sup>29</sup>:

1. Fully permutable *for* loops (order of summations)
2. No dependencies preventing loop fusion
3. A specific index permutation symmetry

A noteworthy effort is the load balancer DLTC<sup>68</sup> which analyzes dependencies between contractions and groups them in layers that can be executed concurrently. This is particularly relevant for higher-order CC with many of contractions of differing workloads.<sup>55</sup>

### C. State-of-the-art: Tensor contraction

Tensor contraction represents the most computer-intensive operation of numerous methods in quantum chemistry, condensed matter physics, nuclear physics, machine learning and quantum computing.<sup>69–71</sup> Examples include coupled cluster methods,<sup>3,72,73</sup> tensor networks,<sup>74</sup> quantum computing simulators<sup>75</sup> and certain neural networks<sup>76</sup> and signal processing methods.<sup>77,78</sup> There, the key limitation to the system size is the cost of tensor contraction.

Typically, the software packages decompose tensor contractions into primitive matrix operations<sup>79,80</sup> and pass them to BLAS. There are different approaches of dealing with tensor transposition (reshape), which is in general required for the usage of GEMM, which depends on a unit-stride index to multiply two matrices. (Note that in this context, the CS community uses the term transposition interchangeably with reshape.) The most common approach is TTGT<sup>70</sup> (Transpose-Transpose-GEMM-Transpose): for  $C = A \times B$

1. Transpose  $A$  and  $B$  into unit-stride form
2. Use GEMM to execute the contraction
3. Transpose result array to obtain  $C$

In his block-scatter matrix tensor contraction (BSMTC) scheme, Matthews<sup>70</sup> has shown that is possible to avoid transposition entirely by loading parts of tensors into CPU L2 and L3 cache in a specific order.

Another alternative is the GETT scheme (GEMM-like tensor-tensor multiplication) by Springer and Bientinesi<sup>81</sup> which generates code to call matrix-matrix multiplication kernels while again reformulating the sub-matrix-packing. A GPU implementation thereof has become a foundation of the proprietary single-node library cuTENSOR.<sup>82</sup>

Regarding the parallelization strategy, most software relies on OpenMP+MPI parallelization on homogenous CPU-based computational clusters.<sup>3</sup> The advent of GPU-based supercomputers has rendered this paradigm obsolete.<sup>73</sup>

Compared to the software for matrix operations, we have identified two major practical hurdles for tensor software:

1. Contrary to BLAS for matrix operations, there is no standardized interface for tensor operations.<sup>69</sup> Currently, there is an ongoing standardization push attempting to find agreement across academia and companies.
2. Contrary to CPU-based software,<sup>41,72</sup> there is no established GPU-based implementation of a tensor contraction library with support for features required by the community such as distributed memory and block sparsity,<sup>73</sup> which would offer sufficient level of maintenance and optimization for current supercomputers.

As for standardization, there has been some work in the past, but none of the interfaces have prevailed. BTAS<sup>79</sup> has aimed at providing a standard and a basic CPU implementation. TBLIS<sup>70</sup> provides BLAS-like tensor calls. Until today, there is no GPU implementation of these. During the Dagstuhl tensor workshop<sup>83</sup> in 2022, a development of domain-specific tensor language has been initiated, but remains unfinished and undocumented. There has been work-technical specifications of additional aspects of standardization, like tensor-memory distribution<sup>84,85</sup> and randomized multilinear algebra.<sup>86</sup>

Regarding the implementations, there are numerous scattered efforts listed in Ref. 69. However, for open-source distributed memory GPU libraries, there is only a few major players. i) ExaTENSOR<sup>6,87</sup> based on TAL-SH<sup>88</sup>, where the key developer has left to industry. ii) TiledArray<sup>72</sup> and Cyclops CTF,<sup>41</sup> where the solid support for GPUs is still under development. iii) TACO DISTAL,<sup>23</sup> which has performance issues for higher-order tensors. iv) TAMM<sup>89</sup> scales well on supercomputers, but has a potentially problematic dependency of Global Arrays,<sup>90</sup> with a small user base for a communication library. v) cuTENSOR<sup>91</sup> is proprietary and only supports Nvidia hardware, while vi) hipTensor<sup>92</sup> is at an early stage of development. Other industry products like vii) PyTorch<sup>93</sup> and viii) TensorFlow<sup>94</sup> focus almost exclusively on machine learning and lack features required by other application domains.

## II. THEORY AND IMPLEMENTATION

### 1. Coupled cluster amplitude equations and their generation

The coupled cluster method is based on an exponential ansatz

$$|CC\rangle = \exp(\hat{T})|\Phi_0\rangle, \quad \hat{T} = \sum_{i=1} t_i \hat{\tau}_i \quad (1)$$

where  $\tau_i$  is the  $i$ -th excitation, and  $t_i$  the corresponding cluster amplitude.  $\Phi_0$  in our case denotes the Hartree Fock (HF) reference.

Even though the code generator is designed to go to arbitrary order and in practice generates optimized code up to CCSDTQP (see Table I), in the presented applications we restrict ourselves to up to quadruple excitations

$$\begin{aligned}\hat{T} &= \hat{T}_1 + \hat{T}_2 + \hat{T}_3 + \hat{T}_4, & \hat{T}_1 &= \sum_{ai} t_i^a a_a^\dagger a_i, \\ \hat{T}_2 &= \frac{1}{4} \sum_{abij} t_{ij}^{ab} a_a^\dagger a_b^\dagger a_j a_i, & \hat{T}_3 &= \frac{1}{36} \sum_{abcijk} t_{ijk}^{abc} a_a^\dagger a_b^\dagger a_c^\dagger a_k a_j a_i, \\ \hat{T}_4 &= \frac{1}{24^2} \sum_{abcdijkl} t_{ijkl}^{abcd} a_a^\dagger a_b^\dagger a_c^\dagger a_d^\dagger a_l a_k a_j a_i.\end{aligned}\quad (2)$$

We use  $i, j, k, l$  and  $a, b, c, d$  to denote occupied and virtual orbitals respectively, whereas  $p, q, r, s$  denotes any orbitals.

After defining the similarity transformed normal-ordered Hamiltonian as  $\bar{H} = \exp(-\hat{T})\hat{H}_N \exp(\hat{T})$ , we can write the CC energy equations

$$\begin{aligned}\langle \Phi_0 | \bar{H} | \Phi_0 \rangle &= E - E_{HF}, \\ \langle \Phi_i | \bar{H} | \Phi_0 \rangle &= 0, \quad i \in \{1, 2, 3, 4\}\end{aligned}\quad (3)$$

which determine the energy and the cluster amplitudes.

The explicit equation terms can then be derived using different techniques. We chose the diagrammatic scheme of Kállay and Surján<sup>36</sup> (see the reasoning in section II A). This general-order coupled cluster derivation scheme is based on a **string representation of CC diagrams**. As depicted in

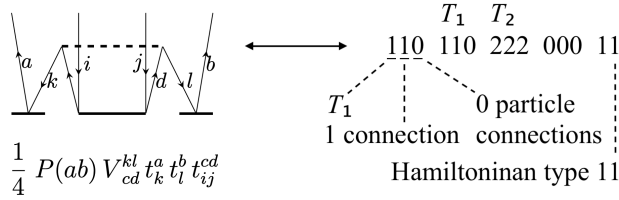


FIG. 2. The string representation of CC diagrams, an example. The three consecutive zeros are to leave space for one further admissible  $\hat{T}$  operator. Note that the triplets of integers corresponding to  $\hat{T}$  operators are ordered to assure uniqueness of the diagrams. See Ref. 36 for a full explanation. Left: Visual representation of a diagram and an equation shown as printed from tenpi.

Scheme 2, integer strings of length 13 is used to represent a diagram. Two diagrams are equivalent up to a sign if their strings are the same. There is a relatively simple algorithm that uses this representation to generate distinct diagrams for each excitation level of the CC Eqs. (3). Please refer to the original Ref. 36 for the full algorithm.

To find the explicit equation terms, tenpi translates the integer strings into line graph representation, i.e. an edge list of particle and hole lines connecting operators and external bra indices of equation Eq. (3). Such a representation makes the application of coupled cluster interpretation rules similar to when done by hand.

### A. Design decisions

The initial goal was to create a programming environment for relativistic coupled cluster which separates science from

the computational platform by getting tensor developments under the hood. This has three aspects:

1. Systematic development of higher-order coupled cluster methods which include hundreds of tensor contractions.
2. Development without having to consider the parallelization strategy.
3. Automatic treatment of tensor symmetries, such as index-permutation symmetry and block-sparsity (for spatially-symmetric systems).

This paper addresses the first two points and prepares the ground for the third point.

The development was driven by practical considerations. The toolchain should not be restricted to a given flavor of the coupled cluster method, but should be written in a general way and be able to go to high orders of the theory. It should allow manipulations of the method by PhD and master students of chemistry. This led to the decision to base the formula generator on **Kucharski-Bartlett diagrams**,<sup>44,45</sup> since diagrams are visual and thus more accessible for students than the other CC derivation schemes (see section I A). The ease of use is one of the reasons why we chose **python** to implement the generator, aside from the fact that it is suitable for text processing and symbolic operations. The **string representation of CC diagrams** of Kállay and Surján<sup>36</sup> was chosen because it can generate distinct connected diagrams and detect equivalent diagrams (see section II 1), both in an efficient and intuitive way.<sup>36</sup>

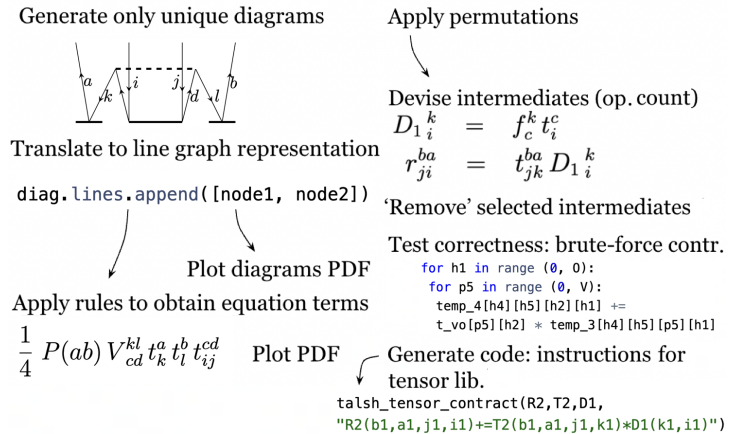


FIG. 3. The workflow of tenpi. First, diagrams are generated. These are then translated to a line chart representation. The CC interpretation rules are applied and both diagrams and equation terms are printed in a textbook-like PDF format. The permutations are applied and resulting code is optimized using OpMin. The produced intermediates are reoptimized to decrease memory cost using the algorithm in Fig. 4. The correctness of intermediates is tested using generated simplistic brute-force python script. Equations are printed in readable format in each of these steps. The entire source code files are generated as required (ExaTENSOR FORTRAN, NumPy python, etc.). The procedure can be fully customized as all these steps are calls to high-level interface of the tenpi python library.

The diagram strings are next translated into **directed graphs**, by storing a list of edges (adjacency matrix). This

representation makes the implementation of the CC interpretation rules readable. Advanced users can define a custom set of rules (customizability) or even extend the Diagram class to allow for multiple interaction operators and other generalizations, without having to change the rest of the code (modularity).

To follow closely the hand-typeset style of the pedagogical texts of Refs. 95 and 44, the toolkit prints the diagrams in PDF format using the CCDiag  $\LaTeX$  package.<sup>96</sup> During the development of higher-order CC methods this **visual representation** proved itself invaluable for debugging.

The flow of the tenpi code generator is depicted in Scheme 3. A key step is to **optimize the expressions** obtained. Since writing a global optimizer from scratch is beyond the scope of this work, we interfaced our code with OpMin, which was chosen due to its favorable performance for higher-order CC.<sup>31</sup> However, for most tests, the FLOP-count based approach of OpMin generates too many intermediates. Higher-order CC tensors in our calculations are too large to be stored on disk due to prohibitive I/O costs. Our approach is to distribute them among the CPU and GPU RAM memory of the nodes. This comes with a limitation in the amount of available distributed memory due to communication overhead growing quadratically with the number of nodes for our simple round-robin distribution scheme. Therefore, we implemented our **own secondary optimization**, which rolls back part of the intermediates by plugging them back in their respective terms. The number of intermediates is reduced by about a factor of three at the expense of increasing the FLOP count (see Fig. 4). This approach is justified as long as the calculation stays communication-dominated. We do not reach a perfect balance, which would require setting up a communication-based cost-function. This is ongoing work.

During the optimization, we originally represented contractions using the SymPy package<sup>97</sup> but later we turned to the use of a **custom representation of tensor contractions** for greater flexibility. Even though SymPy is widely used, its API felt cumbersome for handling higher-order tensors.

The accessibility of the code should not come at the cost of performance. Therefore, the generated production code is strictly in a compiled language, in our case **Fortran 2008** in order to integrate smoothly with the ExaCorr module<sup>87</sup> of the DIRAC package.<sup>98,99</sup>

As we aim for scalability on modern GPU exascale machines, we turned to the use of a **tensor library** to execute the final tensor kernels.

## B. Implementation

An equation term is implemented using the ‘Contraction’ class, which includes a list of tensors, a scalar factor and optionally permutation operators or a result tensor. Contraction class instances are collected in a list, which forms the left-hand side of Eqs. (3).

Tensor class includes a list of upper and lower indices. Each index is an Index class instance. Index class has its type (e.g. occupied, virtual) a convention according to which it

```

1: repeat
2:   if intermediate defined in a single operation then
3:     if it is always used in additions then
4:       plug it back in
5:     end if
6:   end if
7:   if intermediate used only once then
8:     if its definition only contains additions then
9:       plug it back in
10:    else if it is used in an addition then
11:      plug it back in
12:    end if
13:  end if
14: until no change since the last iteration

```

FIG. 4. Secondary optimization of intermediates to help restore the balance between the memory cost and operation count by removing eligible intermediates (plugging them back in the equation). Each time indices have to be permuted accordingly. The scheme is limited by the need to avoid contractions of more than two tensors to keep the instructions compatible with the tensor library.

is printed (e.g.  $a, b, i, j; p_1, p_2, h_1, h_2$ ) and then a number corresponding to order in which the specific character comes in the class (e.g.  $a \mapsto 1, b \mapsto 2, p_1 \mapsto 1$ ). Types and conventions are easily customizable, which is important for the implementation of methods and symmetries with multiple index spaces or tiling.<sup>89</sup> Equations can **switch between conventions** with a single command. This is important because tenpi supports multiple input and output formats to interface with ExaTensor, TAL-SH, OpMin, NumPy, including a possibility to input equations by hand. For the sake of modularity, all these libraries are integrated by extending one of two predefined interfaces: GetCodeInterface or ParseCodeInterface. These specify how to implement a new format of output or input respectively. Thanks to this design it is **straightforward to interface** tenpi with a new program.

The optimization of intermediates is an error-prone procedure and checking the results by hand can be extremely tedious. Therefore, following the example of OpMin, tenpi includes verification of correctness using a generated python brute-force test code with contractions expressed in nested for loops. Random tensors with tiny virtual and occupied sizes are used to check whether the optimized equation produces the same result as the original one.

method	CCD	CCSD	CCSDT	CCSDTQ	CCSDTQP
number of diagrams	11	48	102	183	289
derivation step	0.03 s	0.1 s	0.3 s	0.6 s	0.8 s
intermediates	0.03 s	40 s	22 min	7 h 10 min	4 days 1 h
code generation	0.01 s	0.1 s	3 s	2 min	2 h 13 min

TABLE I. Timings of generation of high-performance code by tenpi, which is itself a sequential python implementation.

The derivation step of tenpi is very fast, see timings in Tab. I. We have verified by comparing with Ref. 36 that tenpi generates the correct number of diagrams of the amplitude equation up to order 20. Even though it generates a highly-parallel

code, tenpi itself is written as sequential python. Despite this, the most demanding step, global intermediate optimization, still performs quite well.

Aside from amplitude equations, tenpi can already generate matrix elements (c.f. SMITH<sup>25,46</sup>) and is currently being extended to generate response density matrices.

During the development, the debugging of CCSDTQ proved quite difficult, due to a mistake in an algorithm generating permutations. A different, simple mistake appeared already at the CCSD level: For the CC diagram interpretation rules to yield a correct sign, e.g. for the case of amplitude-equation projected onto  $|\Phi_{ij}^{ab}\rangle$ , the line starting in  $i$  has to end in  $a$ , and not in  $b$ . This rule is often assumed implicitly.<sup>44,95</sup>

### III. COMPUTATIONAL DETAILS

#### A. Machines used

The calculations were performed on machines listed in Table II which includes their technical specification. When ExaTENSOR,<sup>87</sup> is applied for coupled cluster, the most relevant parameters for the performance are the interconnect bandwidth, RAM (random-access) and HBM (high-bandwidth) memory, and the specification of the GPU. Over the two supercomputer generations represented in the table the bandwidth and HBM have grown about fourfold, while RAM has basically stagnated. Despite the rapid development of GPU processing power, this shows that the evolution of other important parameters has been relatively slow over the last 5 years.

#### B. Relativistic Hamiltonian

The state-of-the-art post-HF four-component relativistic calculations employ the no-pair approximation.<sup>101</sup> This approximation is well-substantiated for applications of chemical scale. Formally, it yields a Hamiltonian analogous to the non-relativistic case

$$H = \sum_{pq} h_p^q a_p^\dagger a_q + \frac{1}{4} \sum_{pqrs} \langle pq||rs \rangle a_p^\dagger a_q^\dagger a_s a_r, \quad (4)$$

where the indices  $p, q, r, s$  run over the positive-energy spinors that span the one-electron basis.

In the present work we employ, unless otherwise stated, the exact two-component (X2C) Hamiltonian, XXX where the summations in Eq. (4) are limited to positive energy orbitals by construction.

Relativistic picture change corrections were added either using the AMFI package CCC or using the more recent amfX2C correction<sup>102</sup>.

#### C. Geometry, basis, etc.

For the bechmarks, we used the UF<sub>6</sub> molecule in dyall.v2z basis<sup>103</sup> with relativistic X2C Hamiltonian, and bond distance of 2.077521 Å. In the corresponding ground-state energy CC calculations, we used a (Dirac-)Hartree-Fock (HF) reference. Despite the high O<sub>h</sub> symmetry, there is no related performance gain in the CC calculations as the implementation does not support it.

Furthermore, we studied CO in cc-pVTZ basis<sup>104</sup> at bond-distances between 0.8 and 1.85 Å. There, we used amfX2C (XAMFI) corrections<sup>102</sup> for scalar-relativistic and spin-orbit two-electron picture-change effects arising within the X2C Hamiltonian framework.<sup>102</sup> HF orbitals for a given point on the curve served as an initial guess for the SCF calculation at the next point with increasing distances.

Then we calculated the MP2 frozen natural orbitals<sup>105</sup> (with a cutoff on occupation number) on top of which the final CC calculation was performed.

We performed two correctness checks with a nonrelativistic Hamiltonian. For the first test, we chose H<sub>2</sub>O in a 3-21G basis<sup>106</sup> at the equilibrium internuclear distance of 0.975512 Å and H-O-H angle of 110.565°. The second test is with LiH in 6-31G basis<sup>107,108</sup> at the internuclear distance of 1.6 Å. Both the CC correctness tests were performed with respect to the HF reference.

All the CC calculations were performed in uncontracted basis sets. When referring to sizes of occupied and virtual spaces, we use the notation of CAS( $k, n$ ), where  $k$  is the number of electrons and  $n$  is the number of Kramers pairs active in a coupled cluster calculation (occupied+virtual). One Kramers pair corresponds to two spinors related by time reversal symmetry. In all calculations, the choice of occupied and virtual spaces respects the rising orbital energies or the occupation numbers in case of MP2. See the used software in section IV A.

### IV. RESULTS AND DISCUSSION

#### A. Correctness: H<sub>2</sub>O and LiH

To demonstrate the correctness, we compare ground state coupled cluster energies from tenpi (present work) with the established MRCC package<sup>36,109-111</sup> and with existing code in DIRAC<sup>98,99</sup> where possible, i.e. either the initial DIRAC RelCC module<sup>112,113</sup> or the recent codegen (mb-autogen).<sup>114</sup> The comparison was performed on two small systems H<sub>2</sub>O (Table III) and LiH (Table IV) and shows an agreement within the convergence thresholds.

#### B. Benchmark: UF<sub>6</sub> CCSD strong scaling

To benchmark the parallel scaling, we compare the performance of CCSD generated by tenpi with hand-tuned code in the ExaCorr module of DIRAC and with generated code from

machine	Frontier	LUMI	Karolina	Summit	Olympe
laboratory organization	OLCF U.S. DOE	CSC data center EuroHPC	IT4Innovations Cz. edu. ministry	OLCF U.S. DOE	CALMIP CNRS
GPU nodes	9408	2978	72	4600	48
GPUs per node	8	8	8	6	4
GPU type	AMD MI250x	AMD MI250x	NVIDIA A100	NVIDIA V100	NVIDIA V100
HBM per GPU	64 GB	64 GB	40 GB	16 GB	16 GB
CPU type	AMD EPYC 7713	AMD EPYC 7A53	AMD EPYC 7452	IBM POWER9	Intel Skylake
cores per node	64	64	64	168	36
RAM per node	512 GB	512 GB	1024 GB	512 GB	384 GB
network	Cray Slingshot	Cray Slingshot-11	Infiniband HDR200	Infiniband EDR	Infiniband EDR
net. bandwidth	4x 25 GB/s	4x 25 GB/s	4x 6.25 GB/s	23 GB/s	12.5 GB/s

TABLE II. GPU-based HPC platforms used for the calculations and their corresponding technical specifications.<sup>100</sup>

method	code	convergence <sup>c</sup>	Total energy [ $E_H$ ]
SCF	DIRAC SCF	1.1E-12 <sup>a</sup>	-75.58 5498 7542
SCF	MRCC	4.4E-13 <sup>a</sup>	-75.58 5498 7680
MP2	DIRAC ExaCorr		-75.66 6586 2130
MP2	MRCC		-75.66 6586 2218
CCSD	DIRAC tenpi <sup>d</sup>	0.5E-09 <sup>c</sup>	-75.67 2947 6512
CCSD	MRCC	9.6E-10 <sup>c</sup>	-75.67 2947 6563
CCSDT	DIRAC tenpi <sup>b</sup>	0.4E-09 <sup>c</sup>	-75.67 3875 1038
CCSDT	MRCC	4.9E-10 <sup>c</sup>	-75.67 3875 1087
CCSDTQ	DIRAC tenpi <sup>b</sup>	0.1E-08 <sup>c</sup>	-75.67 3974 4768
CCSDTQ	MRCC	3.5E-10 <sup>c</sup>	-75.67 3974 4817

TABLE III. Correctness check on the ground state energies of H<sub>2</sub>O. CAS(6, 11). Calculated on Olympe.<sup>a</sup> energy difference<sup>b</sup> using the ExaTENSOR library<sup>c</sup> norm of the residual vector<sup>d</sup> using the single node TAL-SH implementation<sup>e</sup> the final error shown in the run

method	code	convergence <sup>d</sup>	Total energy [ $E_H$ ]
SCF	DIRAC SCF	1.4E-12 <sup>a</sup>	-7.97 9321 5650
SCF	MRCC	6.2E-15 <sup>a</sup>	-7.97 9321 5634
MP2	DIRAC ExaCorr		-7.99 1935 0613
MP2	MRCC		-7.99 1935 0593
CCSD	DIRAC tenpi <sup>b</sup>	0.6E-09 <sup>c</sup>	-7.99 8346 9438
CCSD	MRCC	2.9E-10 <sup>c</sup>	-7.99 8346 9410
CCSDT	DIRAC tenpi <sup>b</sup>	0.5E-09 <sup>c</sup>	-7.99 8358 3476
CCSDT	MRCC	4.2E-10 <sup>c</sup>	-7.99 8358 3449
CCSDTQ	DIRAC tenpi <sup>b</sup>	0.3E-05 <sup>c</sup>	-7.99 8358 3478
CCSDTQ	MRCC	7.0E-10 <sup>c</sup>	-7.99 8358 3630

TABLE IV. Correctness check on LiH. CAS(4, 11). Calculated on Olympe.

<sup>a</sup> energy difference<sup>b</sup> using the ExaTENSOR library<sup>c</sup> norm of the residual vector<sup>d</sup> the final error shown in the run

the codegen (mb-autogen) generator.<sup>114</sup> We perform a strong-scaling benchmark on UF<sub>6</sub>. In all cases, the correct total energy of  $-28638.655880 E_H$  is retrieved with residual norm threshold less than  $0.8 \times 10^{-6}$ . The parallel speedup for strong scaling benchmark is calculated in a standard way as a wall-

time ratio  $t_1/t_N$  for  $N$  processing units (in this case we consider entire nodes). If  $t_1$  is not available due to large memory requirements, the timing per node with the minimal number of nodes is used to estimate it.

The benchmark was performed on the Summit supercomputer of the Oak Ridge Leadership Computing Facility using the GPU implementation of the ExaTENSOR library. Each Summit node is equipped with 6 GPUs (see Table II). We used up to 300 GPUs simultaneously.

As shown in Figure 5, the code scales well until about 20 nodes for UF<sub>6</sub>. There, the curve leaves its approximately linear behaviour. This is expected as the internode communication overhead increases with the number of nodes. This can be modelled via Amdahl’s law<sup>115</sup> for strong scaling with the timing proportion of ‘serial code’ at 5.5% when the processes wait for communication during tensor operations and for synchronization barriers which are enforced after each tensor operation.

As expected, the automatically generated code is slightly less efficient than the hand-tuned code. The timings in Figure 6 show a fixed-factor slowdown of about 30% for tenpi, whereas about 80% for codegen. The former is a good result when compared with ORCA, where 100% timing overhead was a practical rule of thumb threshold for acceptance of generated code.<sup>12</sup>

### C. Application: CO

The study of the CO molecule was chosen as an application, due to the interesting aspects of its triple bond stretching, studied in a recent work by the Shabaev group.<sup>116</sup> There, the influence of quantum electrodynamics (QED) corrections is analyzed which is relevant for the HAMP-vQED project<sup>117</sup> for which the present code was created. These are small-scale effects and their study requires highly accurate methods.

We used the recently implemented amfX2C (XAMFI) correction<sup>102</sup> for relativistic picture-change effects.

Fig. 7 shows the ground state energies up to the CCSDT level for the bond distance stretching from 0.8 to 1.85 Å. Fig. 8 shows similar results for up to CCSDTQ level with a smaller space.

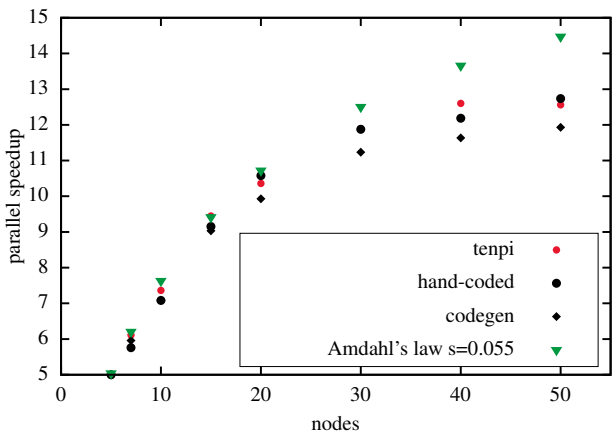


FIG. 5. Strong scaling benchmark on  $\text{UF}_6$ . Average parallel speedup for a relativistic CCSD iteration (relative to the smallest possible run) with respect to the number of Summit nodes (6 GPUs per node). CAS(66,190).

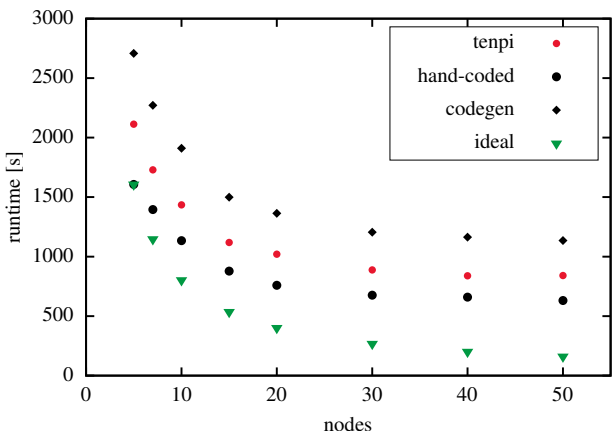


FIG. 6. Strong scaling benchmark on  $\text{UF}_6$ . Average timing of a relativistic CCSD iteration with respect to the number of Summit nodes (6 GPUs per node). CAS(66,190).

As expected, single-reference methods struggle for large bond distances. The nonparallelity of CCSD and CCSDT becomes apparent at the bond distance of  $1.75 \text{ \AA}$  (Fig. 7) and the CC has convergence issues from  $1.85 \text{ \AA}$  on. This is also visible for the rightmost two points for CCSDTQ in Fig. 8.

A deeper study of the behavior of higher-order CC upon dissociation, and especially finding the minimum CC excitation level to break the bond successfully is beyond the scope of this manuscript, and will be a subject for our further work. Furthermore, we will study how amfX2C and QED corrections influence the result.

## V. CONCLUSIONS

The code generated from tenpi represents the first implementation of CCSDT and CCSDTQ in DIRAC. For massively

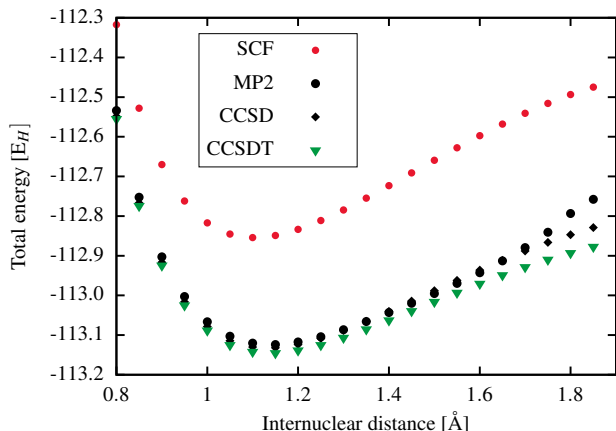


FIG. 7. Carbon monoxide ground state energy, CAS(10,40), X2C Hamiltonian with amfX2C correction. Calculated on Frontier.

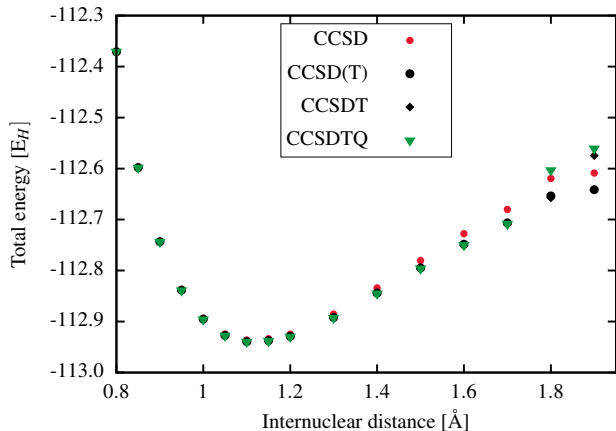


FIG. 8. Carbon monoxide ground state energy, CAS(12,10), X2C Hamiltonian with amfX2C correction. Calculated on Frontier.

parallel CCSD, it shows a performance comparable to the hand-tuned code with the measured overhead of only 30%, which is an improvement over the 80% overhead of the existing generated CCSD.

Overall, tenpi provides users with an elegant and systematic way of implementing the coupled cluster methods while hiding under the hood most of the complexity related to the equations, parallelization and intermediates. A simple python interface is featured, while the output is a highly optimized Fortran code that controls the parallel tensor library.

The stretching of the triple bond of CO was studied with convergence problems observed for higher-order CC, particularly for CCSDTQ at larger bond distances.

The outlook for tenpi includes the development of CCSD(T) and CCSDT(Q) for distributed-GPU platforms, implementation of spatial-symmetry support, and the integration of DIRAC with new tensor software. Improvement of intermediate optimization for these applications can be studied and the impact on internode communication minimized. The method development can be boosted by a symbolic interface to Mathematica. tenpi can also serve as a standalone produc-



tion CC package, if the integral generation is interfaced directly to an existing code, like ReSpect.<sup>118</sup>

## ACKNOWLEDGMENTS

We very much acknowledge the consultations and support from André S.P. Gomes, Dmitry Lyakh, Jiří Pittner, Marcus Wagner, Lucas Visscher, Gabriele Fabbro and Paolo Bientinesi. This project has received funding from the the European Research Council (ERC) under the European Union’s Horizon 2020 research and innovation programme (grant agreement No 101019907). This research used resources of the Oak Ridge Leadership Computing Facility at the Oak Ridge National Laboratory, which is supported by the Office of Science of the U.S. Department of Energy under Contract No. DE-AC05-00OR22725. This work was granted access to the HPC resources of CALMIP supercomputing center under the allocation 2023-p13154 and 2024-M24070. We acknowledge VSB – Technical University of Ostrava, IT4Innovations National Supercomputing Center, Czech Republic, for awarding this project access to the LUMI supercomputer, owned by the EuroHPC Joint Undertaking, hosted by CSC (Finland) and the LUMI consortium through the Ministry of Education, Youth and Sports of the Czech Republic through the e-INFRA CZ (grant ID: 90254). We acknowledge the use of the MRCC package<sup>109,110</sup> and its CC methods.<sup>36,111</sup>

<sup>1</sup>J. Dongarra, “A Not So Simple Matter of Software,” (2023).

<sup>2</sup>F. Chirigati, *Nature Computational Science* **2**, 211–212 (2022).

<sup>3</sup>J. A. Calvin, C. Peng, V. Rishi, A. Kumar, and E. F. Valeev, *Chemical Reviews* **121**, 1203 (2021).

<sup>4</sup>W. Ma, S. Krishnamoorthy, and G. Agrawal, “Practical Loop Transformations for Tensor Contraction Expressions on Multi-level Memory Hierarchies,” in *Compiler Construction* (Springer Berlin Heidelberg, 2011) p. 266–285.

<sup>5</sup>C. Woolston, “Why science needs more research software engineers,” (2022).

<sup>6</sup>D. I. Lyakh, *International Journal of Quantum Chemistry* **119**, (2019).

<sup>7</sup>S. Thibault, *On Runtime Systems for Task-based Programming on Heterogeneous Platforms*, *Habilitation à diriger des recherches*, Université de Bordeaux (2018).

<sup>8</sup>E. Rojas, E. Meneses, T. Jones, and D. Maxwell, in *2019 31st International Symposium on Computer Architecture and High Performance Computing (SBAC-PAD)* (IEEE, 2019).

<sup>9</sup>D. Zhao, S. Samsi, J. McDonald, B. Li, D. Bestor, M. Jones, D. Tiwari, and V. Gadepally, in *Proceedings of the 2023 ACM Symposium on Cloud Computing*, SoCC ’23 (ACM, 2023).

<sup>10</sup>T. A. Heffernan and A. McKay, *Professional Development in Education* **45**, 102–113 (2018).

<sup>11</sup>“Summit User Guide,” [https://docs.olcf.ornl.gov/systems/summit\\_user\\_guide.html](https://docs.olcf.ornl.gov/systems/summit_user_guide.html) (2024), [Online; accessed 27-May-2024].

<sup>12</sup>M. H. Lechner, A. Papadopoulos, K. Sivalingam, A. A. Auer, A. Koslowski, U. Becker, F. Wennmohs, and F. Neese, *Physical Chemistry Chemical Physics* **26**, 15205–15220 (2024).

<sup>13</sup>A. Papadopoulos, “Necessity of Code Generators in Electronic-Structure Theories and their Infrastructure,” (2019).

<sup>14</sup>A. A. Auer, G. Baumgartner, D. E. Bernholdt, A. Bibireata, V. Choppella, D. Cociorva, X. Gao, R. Harrison, S. Krishnamoorthy, S. Krishnan, C.-C. Lam, Q. Lu, M. Nooijen, R. Pitzer, J. Ramanujam, P. Sadayappan, and A. Sibiryakov, *Molecular Physics* **104**, 211–228 (2006).

<sup>15</sup>The Mathworks, Inc., “MATLAB,” (2024).

<sup>16</sup>Waterloo Maple, Inc., “Maple,” (2024).

<sup>17</sup>W. R. Inc., “Mathematica, Version 14.0,” (2024), champaign, IL, 2024.

<sup>18</sup>The Chronos Group, Inc., “SYCL,” (2021).

<sup>19</sup>The OpenACC Organization, “OpenACC,” (2022).

<sup>20</sup>C. Augonnet, S. Thibault, R. Namyst, and P.-A. Wacrenier, *Concurrency and Computation: Practice and Experience Euro-Par 2009 best papers*, **23**, 187 (2011).

<sup>21</sup>R. J. Harrison, G. Beylkin, F. A. Bischoff, J. A. Calvin, G. I. Fann, J. Fosso-Tande, D. Galindo, J. R. Hammond, R. Hartman-Baker, J. C. Hill, J. Jia, J. S. Kottmann, M.-J. Yvonne Ou, J. Pei, L. E. Ratcliff, M. G. Reuter, A. C. Richie-Halford, N. A. Romero, H. Sekino, W. A. Shelton, B. E. Sundahl, W. S. Thornton, E. F. Valeev, A. Vazquez-Mayagoitia, N. Vence, T. Yanai, and Y. Yokoi, *SIAM Journal on Scientific Computing* **38**, S123–S142 (2016).

<sup>22</sup>M. Bauer, S. Treichler, E. Slaughter, and A. Aiken, in *2012 International Conference for High Performance Computing, Networking, Storage and Analysis* (IEEE, 2012).

<sup>23</sup>R. Yadav, A. Aiken, and F. Kjolstad, in *Proceedings of the 43rd ACM SIGPLAN International Conference on Programming Language Design and Implementation* (ACM, 2022).

<sup>24</sup>A. D. Bochevarov, E. F. Valeev, and C. David SheRrill, *Molecular Physics* **102**, 111–123 (2004).

<sup>25</sup>T. Shiozaki, M. Kamiya, S. Hirata, and E. F. Valeev, *Physical Chemistry Chemical Physics* **10**, 3358 (2008).

<sup>26</sup>V. Lotrich, N. Flocke, M. Ponton, B. A. Sanders, E. Deumens, R. J. Bartlett, and A. Perera, in *Proceedings of the 23rd international conference on Supercomputing*, ICS ’09 (ACM, 2009).

<sup>27</sup>D. A. Matthews, *Molecular Physics* **117**, 1325–1333 (2018).

<sup>28</sup>L. Zheng *et al.*, “Awesome Tensor Compilers,” <https://github.com/merrymercy/awesome-tensor-compilers> (2024).

<sup>29</sup>A. Panyala, *Search-based Model-driven Loop Optimizations for Tensor Contractions*, *Ph.D. thesis*, Louisiana State University Libraries (2014).

<sup>30</sup>J. Brandejs, P. Bientinesi, L. Visscher, A. Gomes, T. Saue, *et al.*, “CECAM Workshop on Tensor Contraction Library Standardization,” (2024).

<sup>31</sup>P.-W. Lai, H. Zhang, S. Rajbhandari, E. Valeev, K. Kowalski, and P. Sadayappan, *Proceedia Computer Science* **9**, 412–421 (2012).

<sup>32</sup>G. Baumgartner, A. Auer, D. Bernholdt, A. Bibireata, V. Choppella, D. Cociorva, X. Gao, R. Harrison, S. Hirata, S. Krishnamoorthy, S. Krishnan, C.-C. Lam, Q. Lu, M. Nooijen, R. Pitzer, J. Ramanujam, P. Sadayappan, and A. Sibiryakov, *Proceedings of the IEEE* **93**, 276–292 (2005).

<sup>33</sup>R. A. Kendall, E. Aprà, D. E. Bernholdt, E. J. Bylaska, M. Dupuis, G. I. Fann, R. J. Harrison, J. Ju, J. A. Nichols, J. Nieplocha, T. Straatsma, T. L. Windus, and A. T. Wong, *Computer Physics Communications* **128**, 260–283 (2000).

<sup>34</sup>C. L. Janssen and H. F. Schaefer, *Theoretica Chimica Acta* **79**, 1–42 (1991).

<sup>35</sup>X. Li and J. Paldus, *The Journal of Chemical Physics* **101**, 8812–8826 (1994).

<sup>36</sup>M. Kállay and P. R. Surján, *The Journal of Chemical Physics* **115**, 2945–2954 (2001).

<sup>37</sup>M. Nooijen and V. Lotrich, *Journal of Molecular Structure: THEOCHEM* **547**, 253–267 (2001).

<sup>38</sup>E. Deumens, V. F. Lotrich, A. S. Perera, R. J. Bartlett, N. Jindal, and B. A. Sanders, “The Super Instruction Architecture,” in *Annual Reports in Computational Chemistry* (Elsevier, 2011) p. 179–191.

<sup>39</sup>Y. Shao, L. F. Molnar, Y. Jung, J. Kusmann, C. Ochsenfeld, S. T. Brown, A. T. Gilbert, L. V. Slipchenko, S. V. Levchenko, D. P. O’Neill, R. A. DiStasio Jr, R. C. Lochan, T. Wang, G. J. Beran, N. A. Besley, J. M. Herbert, C. Yeh Lin, T. Van Voorhis, S. Hung Chien, A. Sodt, R. P. Steele, V. A. Rassolov, P. E. Maslen, P. P. Korambath, R. D. Adamson, B. Austin, J. Baker, E. F. C. Byrd, H. Dachsel, R. J. Doerksen, A. Dreuw, B. D. Dunietz, A. D. Dutoi, T. R. Furlani, W. R. Gwaltney, A. Heyden, S. Hirata, C.-P. Hsu, G. Kedziora, R. Z. Khallilulin, P. Klunzinger, A. M. Lee, M. S. Lee, W. Liang, I. Lotan, N. Nair, B. Peters, E. I. Proynov, P. A. Pieniazek, Y. Min Rhee, J. Ritchie, E. Rosta, C. D. Sherrill, A. C. Simmonett, J. E. Subotnik, H. Lee Woodcock III, W. Zhang, A. T. Bell, A. K. Chakraborty, D. M. Chipman, F. J. Keil, A. Warshel, W. J. Hehre, H. F. Schaefer III, J. Kong, A. I. Krylov, P. M. W. Gill, and M. Head-Gordon, *Phys. Chem. Chem. Phys.* **8**, 3172–3191 (2006).

<sup>40</sup>E. Epifanovsky, M. Wormit, T. Kuš, A. Landau, D. Zuev, K. Khistyayev, P. Manohar, I. Kaliman, A. Dreuw, and A. I. Krylov, *Journal of Computational Chemistry* **34**, 2293–2309 (2013).

<sup>41</sup>E. Solomonik, D. Matthews, J. Hammond, and J. Demmel, in *2013*

- IEEE 27th International Symposium on Parallel and Distributed Processing* (IEEE, 2013).
- 42 J. A. Calvin, C. A. Lewis, and E. F. Valeev, in *Proceedings of the 5th Workshop on Irregular Applications: Architectures and Algorithms*, SC15 (ACM, 2015).
  - 43 A. Irmiler, R. Kanakagiri, S. T. Ohlmann, E. Solomonik, and A. Grüneis, “Optimizing Distributed Tensor Contractions Using Node-Aware Processor Grids,” in *Euro-Par 2023: Parallel Processing* (Springer Nature Switzerland, 2023) p. 710–724.
  - 44 I. Shavitt and R. J. Bartlett, *Many-Body Methods in Chemistry and Physics: MBPT and Coupled-Cluster Theory* (Cambridge University Press, 2009).
  - 45 S. A. Kucharski and R. J. Bartlett, *The Journal of Chemical Physics* **97**, 4282–4288 (1992).
  - 46 T. Shiozaki, *WIREs Computational Molecular Science* **8**, (2017).
  - 47 J. Goldstone, *Proceedings of the Royal Society of London. Series A. Mathematical and Physical Sciences* **239**, 267–279 (1957).
  - 48 J. W. Park and T. Shiozaki, *Journal of Chemical Theory and Computation* **13**, 3676–3683 (2017).
  - 49 F. Neese, *WIREs Computational Molecular Science* **12** (2022), 10.1002/wcms.1606.
  - 50 M. Krupička, K. Sivalingam, L. Huntington, A. A. Auer, and F. Neese, *Journal of Computational Chemistry* **38**, 1853–1868 (2017).
  - 51 R. Song, T. M. Henderson, and G. E. Scuseria, *The Journal of Chemical Physics* **156**, (2022).
  - 52 M. Saitow, Y. Kurashige, and T. Yanai, *The Journal of Chemical Physics* **139**, (2013).
  - 53 E. Neuscamman, T. Yanai, and G. K.-L. Chan, *The Journal of Chemical Physics* **130**, (2009).
  - 54 A. Köhn, G. W. Richings, and D. P. Tew, *The Journal of Chemical Physics* **129**, (2008).
  - 55 E. Solomonik, D. Matthews, J. R. Hammond, J. F. Stanton, and J. Demmel, *Journal of Parallel and Distributed Computing* **74**, 3176–3190 (2014).
  - 56 D. G. A. Smith and J. Gray, *Journal of Open Source Software* **3**, 753 (2018).
  - 57 R. Quintero-Monsebaiz and P.-F. Loos, *AIP Advances* **13**, (2023).
  - 58 D. I. Lyakh, V. V. Ivanov, and L. Adamowicz, *The Journal of Chemical Physics* **122**, (2004).
  - 59 L. Chi-Chung, P. Sadayappan, and R. Wenger, *Parallel Processing Letters* **07**, 157–168 (1997).
  - 60 L. Ma, J. Ye, and E. Solomonik, in *Proceedings of the ACM International Conference on Parallel Architectures and Compilation Techniques*, PACT ’20 (ACM, 2020).
  - 61 A. Harju, T. Siro, F. F. Canova, S. Hakala, and T. Rantalaiho, “Computational Physics on Graphics Processing Units,” in *Lecture Notes in Computer Science* (Springer Berlin Heidelberg, 2013) p. 3–26.
  - 62 X. Gao, S. Krishnamoorthy, S. K. Sahoo, C.-C. Lam, G. Baumgartner, J. Ramanujam, and P. Sadayappan, “Efficient Search-Space Pruning for Integrated Fusion and Tiling Transformations,” in *Lecture Notes in Computer Science* (Springer Berlin Heidelberg, 2006) p. 215–229.
  - 63 S. Sahoo, S. Krishnamoorthy, R. Panuganti, and P. Sadayappan, in *ACM/IEEE SC 2005 Conference (SC’05)* (IEEE, 2005).
  - 64 R. Yadav, M. Bauer, D. Broman, M. Garland, A. Aiken, and F. Kjolstad, “Automatic Tracing in Task-Based Runtime Systems,” (2024).
  - 65 J. Johnson, R. W. Johnson, D. A. Padua, and J. Xiong, “Searching for the Best FFT Formulas with the SPL Compiler,” in *Lecture Notes in Computer Science* (Springer Berlin Heidelberg, 2001) p. 112–126.
  - 66 E. Meiron, H. Maron, S. Mannor, and G. Chechik, in *International Conference on Machine Learning* (PMLR, 2022) pp. 15278–15292.
  - 67 U. Bondhugula, A. Hartono, J. Ramanujam, and P. Sadayappan, *ACM SIGPLAN Notices* **43**, 101–113 (2008).
  - 68 P.-W. Lai, K. Stock, S. Rajbhandari, S. Krishnamoorthy, and P. Sadayappan, in *Proceedings of the International Conference on High Performance Computing, Networking, Storage and Analysis*, SC13 (ACM, 2013).
  - 69 C. Psarras, L. Karlsson, J. Li, and P. Bientinesi, “The landscape of software for tensor computations,” (2021).
  - 70 D. A. Matthews, *SIAM Journal on Scientific Computing* **40**, C1 (2018).
  - 71 J. Brabec, J. Brandejs, K. Kowalski, S. Xantheas, O. Legeza, and L. Veis, *Journal of Computational Chemistry* **42**, 534–544 (2020).
  - 72 C. Peng, J. A. Calvin, F. Pavošević, J. Zhang, and E. F. Valeev, *The Journal of Physical Chemistry A* **120**, 10231 (2016).
  - 73 T. Heralut, Y. Robert, G. Bosilca, R. J. Harrison, C. A. Lewis, E. F. Valeev, and J. J. Dongarra, in *2021 IEEE International Parallel and Distributed Processing Symposium (IPDPS)* (IEEE, 2021).
  - 74 R. Levy, E. Solomonik, and B. K. Clark, in *SC20: International Conference for High Performance Computing, Networking, Storage and Analysis* (IEEE, 2020).
  - 75 D. I. Lyakh, T. Nguyen, D. Claudino, E. Dumitrescu, and A. J. McCaskey, *Frontiers in Applied Mathematics and Statistics* **8**, (2022).
  - 76 O. Sharir, A. Shashua, and G. Carleo, *Physical Review B* **106**, (2022).
  - 77 E. C. Chi and T. G. Kolda, *SIAM Journal on Matrix Analysis and Applications* **33**, 1272 (2012).
  - 78 N. D. Sidiropoulos, L. D. Lathauwer, X. Fu, K. Huang, E. E. Papalexakis, and C. Faloutsos, *IEEE Transactions on Signal Processing* **65**, 3551 (2017).
  - 79 Y. Shi, U. N. Niranjan, A. Anandkumar, and C. Cecka, in *2016 IEEE 23rd International Conference on High Performance Computing (HiPC)* (IEEE, 2016).
  - 80 E. Georganas, D. Kalamkar, S. Avancha, M. Adelman, C. Anderson, A. Breuer, J. Bruestle, N. Chaudhary, A. Kundu, D. Kutnick, F. Laub, V. Md, S. Misra, R. Mohanty, H. Pabst, B. Ziv, and A. Heinecke, in *Proceedings of the International Conference for High Performance Computing, Networking, Storage and Analysis* (ACM, 2021).
  - 81 P. Springer and P. Bientinesi, “Design of a high-performance GEMM-like Tensor-Tensor Multiplication,” (2016).
  - 82 “NVIDIA cuTENSOR: A High-Performance CUDA Library For Tensor Primitives,” (2019).
  - 83 P. Bientinesi, D. Ham, F. Huang, P. H. J. Kelly, P. S. Sadayappan, and E. Stow, *Dagstuhl Reports*, (2022).
  - 84 E. Valeev, “Basic Programming of TiledArray,” [https://valeevgroup.github.io/tiledarray/dox-master/\\_basic-\\_programming.html](https://valeevgroup.github.io/tiledarray/dox-master/_basic-_programming.html) (2023), [Online; accessed 13-July-2023].
  - 85 cppreference.com community, “C++ reference MDSPAN,” <https://en.cppreference.com/w/cpp/container/mdspan> (2023), [Online; accessed 13-July-2023].
  - 86 R. Murray, J. Demmel, M. W. Mahoney, N. B. Erichson, M. Melnichenko, O. A. Malik, L. Grigori, P. Luszczek, M. Dereziński, M. E. Lopes, T. Liang, H. Luo, and J. Dongarra, “Randomized Numerical Linear Algebra: A Perspective on the Field With an Eye to Software,” (2023), arXiv.
  - 87 J. V. Pototschnig, A. Papadopoulos, D. I. Lyakh, M. Repisky, L. Halbert, A. S. P. Gomes, H. J. Aa. Jensen, and L. Visscher, *Journal of Chemical Theory and Computation* **17**, 5509 (2021).
  - 88 “TAL-SH,” (2018).
  - 89 E. Mutlu, A. Panyala, N. Gawande, A. Bagussetty, J. Glabe, J. Kim, K. Kowalski, N. P. Bauman, B. Peng, H. Pathak, J. Brabec, and S. Krishnamoorthy, *The Journal of Chemical Physics* **159**, (2023).
  - 90 B. Palmer, E. Apra, A. Panyala, J. Hammond, C. Pe, and S. Krishnamoorthy, “GlobalArrays,” <https://github.com/GlobalArrays/ga> (2022).
  - 91 T. Zhang, X.-Y. Liu, X. Wang, and A. Walid, *IEEE Transactions on Parallel and Distributed Systems* **31**, 595 (2020).
  - 92 C. Millette, C. Ma, and M. Karunanidhi, “hipTensor,” <https://github.com/ROCm/hipTensor> (2024).
  - 93 A. Paszke, S. Gross, F. Massa, A. Lerer, J. Bradbury, G. Chanan, T. Killeen, Z. Lin, N. Gimelshein, L. Antiga, A. Desmaison, A. Kopf, E. Yang, Z. DeVito, M. Raison, A. Tejani, S. Chilamkurthy, B. Steiner, L. Fang, J. Bai, and S. Chintala, in *Advances in Neural Information Processing Systems 32* (Curran Associates, Inc., 2019) pp. 8024–8035.
  - 94 M. Abadi, in *Proceedings of the 21st ACM SIGPLAN International Conference on Functional Programming* (ACM, 2016).
  - 95 T. D. Crawford and H. F. Schaefer, *Reviews in Computational Chemistry* **14**, 33 (2000).
  - 96 D. Kats, “CCDiag - Coupled-Cluster diagrams in LaTeX,” <https://github.com/fkfest/ccdiag> (2024).
  - 97 A. Meurer, C. P. Smith, M. Paprocki, O. Čertík, S. B. Kirpichev, M. Rocklin, A. Kumar, S. Ivanov, J. K. Moore, S. Singh, T. Rathnayake, S. Vig, B. E. Granger, R. P. Muller, F. Bonazzi, H. Gupta, S. Vats, F. Johansson, F. Pedregosa, M. J. Curry, A. R. Terrel, v. Roučka, A. Saboo, I. Fernando, S. Kulal, R. Cimrman, and A. Scopatz, *PeerJ Computer Science* **3**, e103 (2017).
  - 98 L. Visscher, H. J. Aa. Jensen, R. Bast, A. S. P. Gomes, T. Saue, I. A.

- Aucar, V. Bakken, J. Brandeys, C. Chibueze, J. Creutzberg, K. G. Dyall, S. Dubillard, U. Ekström, E. Eliav, T. Enevoldsen, E. Faßhauer, T. Fleig, O. Fossgaard, L. Halbert, E. D. Hedegård, T. Helgaker, B. Helmich-Paris, J. Henriksson, M. van Horn, M. Iliaš, C. R. Jacob, S. Knecht, S. Komorovský, O. Kullie, J. K. Lærdahl, C. V. Larsen, Y. S. Lee, N. H. List, H. S. Nataraj, M. K. Nayak, P. Norman, A. Nyvang, M. Olejniczak, J. Olsen, J. M. H. Olsen., A. Papadopoulos, Y. C. Park, J. K. Pedersen, M. Pernpointner, J. V. Pototschnig, R. Di Remigio Eikås, M. Repiský, K. Ruud, P. Salek, B. Schimmelpfennig, B. Senjean, A. Shee, J. Sikkema, A. Sunaga, J. Thyssen, J. van Stralen, M. L. Vidal, S. Villaume, O. Visser, T. Winther, S. Yamamoto, and X. Yuan, “**DIRAC24**,” (2024).
- <sup>99</sup>T. Saue, R. Bast, A. S. P. Gomes, H. J. Aa. Jensen, L. Visscher, I. A. Aucar, R. Di Remigio, K. G. Dyall, E. Eliav, E. Fasshauer, T. Fleig, L. Halbert, E. D. Hedegård, B. Helmich-Paris, M. Iliaš, C. R. Jacob, S. Knecht, J. K. Laerdahl, M. L. Vidal, M. K. Nayak, M. Olejniczak, J. M. H. Olsen, M. Pernpointner, B. Senjean, A. Shee, A. Sunaga, and J. N. P. van Stralen, *The Journal of Chemical Physics* **152**, (2020).
- <sup>100</sup>TOP500.org, “TOP500 list,” <https://www.top500.org> (2024), [Online; accessed 06-Sep-2024].
- <sup>101</sup>K. G. Dyall and K. Faegri, *Introduction to Relativistic Quantum Chemistry* (Oxford University Press, 2007).
- <sup>102</sup>S. Knecht, M. Repisky, H. J. Aa. Jensen, and T. Saue, *The Journal of Chemical Physics* **157**, (2022).
- <sup>103</sup>K. G. Dyall, “Dyall dz, tz, and qz basis sets for relativistic electronic structure calculations,” (2023).
- <sup>104</sup>T. H. Dunning, *J. Chem. Phys.* **90**, 1007 (1989).
- <sup>105</sup>X. Yuan, L. Visscher, and A. S. P. Gomes, *The Journal of Chemical Physics* **156**, (2022).
- <sup>106</sup>J. S. Binkley, J. A. Pople, and W. J. Hehre, *J. Am. Chem. Soc.* **102**, 939 (1980).
- <sup>107</sup>J. D. Dill and J. A. Pople, *J. Chem. Phys.* **62**, 2921 (1975).
- <sup>108</sup>R. Ditchfield, W. J. Hehre, and J. A. Pople, *J. Chem. Phys.* **54**, 724 (1971).
- <sup>109</sup>M. Kállay, P. R. Nagy, D. Mester, Z. Rolik, G. Samu, J. Csontos, J. Csóka, P. B. Szabó, L. Gyevi-Nagy, B. Hégyely, I. Ladjánszki, L. Szegedy, B. Ladóczki, K. Petrov, M. Farkas, P. D. Mezei, and Á. Ganyecz, *J. Chem. Phys.* **152**, 074107 (2020).
- <sup>110</sup>“**MRCC**,” (2024), MRCC, a quantum chemical program suite written by M. Kállay, P. R. Nagy, D. Mester, L. Gyevi-Nagy, J. Csóka, P. B. Szabó, Z. Rolik, G. Samu, J. Csontos, B. Hégyely, Á. Ganyecz, I. Ladjánszki, L. Szegedy, B. Ladóczki, K. Petrov, M. Farkas, P. D. Mezei, and R. A. Horváth. See [www.mrcc.hu](http://www.mrcc.hu).
- <sup>111</sup>M. Kállay, J. Gauss, and P. G. Szalay, *The Journal of Chemical Physics* **119**, 2991–3004 (2003).
- <sup>112</sup>L. Visscher, T. J. Lee, and K. G. Dyall, *The Journal of Chemical Physics* **105**, 8769–8776 (1996).
- <sup>113</sup>A. Shee, L. Visscher, and T. Saue, *The Journal of Chemical Physics* **145**, (2016).
- <sup>114</sup>A. Gomes and D. I. Lyakh, “**Relmbdev/mb-autogen: mb-autogen**,” (2023).
- <sup>115</sup>G. M. Amdahl, *Computer* **46**, 38–46 (2013).
- <sup>116</sup>D. P. Usov, Y. S. Kozhedub, V. V. Meshkov, A. V. Stolyarov, N. K. Dulaev, A. M. Ryzhkov, I. M. Savelyev, V. M. Shabaev, and I. I. Tupitsyn, *Physical Review A* **109**, (2024).
- <sup>117</sup>T. Saue *et al.*, “**HAMP-vQED**,” (2024).
- <sup>118</sup>M. Repisky, S. Komorovsky, M. Kadek, L. Konecny, U. Ekström, E. Malkin, M. Kaupp, K. Ruud, O. L. Malkina, and V. G. Malkin, *The Journal of Chemical Physics* **152**, (2020).